THE ASTROPHYSICAL JOURNAL, 334:539–551, 1988 November 15

THE GASDYNAMICS OF COMPACT RELATIVISTIC JETS

RUTH A. DALY[1] AND ALAN P. MARSCHER
Department of Astronomy, Boston University
Received 1987 October 26; accepted 1988 May 2

ABSTRACT

We explore the gasdynamics of compact relativistic jets by analyzing a specific idealized flow problem using the method of characteristics. The basic flow pattern of the gas and pressure waves within a jet experiencing a drop in external pressure is calculated, with analytic expressions given for many of the important parameters. Scaling laws which relate the intrinsic properties of the jet to the pressure of the surrounding medium are obtained and discussed. The physical properties of the jet depend critically on the value and abruptness of the decrease in external pressure, as well as on the initial Lorentz factor of the flow. A variety of flow patterns can result, including jets of oscillating cross section, jets with standing shocks, and broad, nearly hollow beams which can break up into multiple jets. These results are discussed in relation to the observed characteristics of superluminal radio sources in general and the superluminal quasar 4C 39.25 in particular.

Subject headings: galaxies: jets — hydrodynamics — quasars — relativity

I. INTRODUCTION

Observations of apparent superluminal motion, rapid brightness changes, high brightness temperatures, and one-sided, bent jets in compact radio sources have been modeled successfully in terms of relativistic plasma jets emanating from the central regions of quasars and active galactic nuclei (Blandford and Rees 1978; Blandford and Königl 1979; Königl 1981; Reynolds and McKee 1980; Marscher 1980). Most specific models of jet emission (e.g., Königl 1981; Marscher and Gear 1985) have thus far adopted a simple conical geometry for the jet and assumed a constant flow velocity. Such simple assumptions serve to reduce the number of free parameters, thereby making the problem tractable. Nevertheless, as has been shown dramatically for nonrelativistic jets by Norman, Winkler, and Smarr (1983), the dynamics of jets can lead to a wide variety of flow patterns. In this study we analyze the dynamics of jets with internal energy densities which are ultrarelativistic in the proper frame of each fluid element. We use the method of characteristics to calculate the flow pattern as well as variations in the physical properties of the fluid as functions of position in the jet. Since the method of characteristics does not allow one to calculate the flow pattern across shocks, this work is but a first step in a broader study of relativistic jet dynamics. Nevertheless, we discuss qualitatively how the presence of shocks affects the observed properties of compact jets.

In § II we show how the characteristic equations describing two- and three-dimensional, axisymmetric, relativistic flows of gas described by a relativistic equation of state are obtained. These characteristic equations may be solved numerically to obtain the shape of the jet boundary and state of the gas at points within the jet once the boundary conditions have been specified. By studying the numerical solutions to the characteristic equations for a full range of boundary conditions, we obtain the dependence of the solutions on the boundary conditions. This allows us to determine analytic approximations (or "scaling laws") which describe the gross physical characteristics parameterizing an arbitrary jet as a function of the boundary conditions; these scaling laws are presented in § III. Using these analytic approximations, many properties of a jet may be deduced once the boundary conditions are specified. Conversely, if some of the jet properties may be deduced or inferred from observations, the scaling laws presented in § III may be used to determine the boundary conditions (i.e. to determine the pressure of the medium confining the jet and/or the initial Lorentz factor of the flow). A discussion of how these results may be applied to jets is given in § IV. In this section we also discuss qualitatively how the theoretical dynamics of relativistic jets might apply to models of compact radio jets as observed with very long baseline interferometry (VLBI). The conclusions follow in § V.

II. PROCEDURE

We illustrate the flow properties of a relativistic jet by considering a classical idealized flow problem: a cylindrically symmetric jet of relativistic particles and dynamically weak, frozen-in magnetic field is confined by and in pressure equilibrium with its surroundings (the external pressure). At some point the external pressure drops to a lower value. The desired results of the calculation are the shape of the boundary of the jet and the bulk flow velocity, pressure, and internal energy of the gas within the jet as a function of position.

We begin with the general equations of motion for a fluid. The fluid is moving with three-velocity v and bulk Lorentz factor Γ relative to a stationary (lab) frame. In the rest frame of the fluid the gas is relativistic and is therefore described by the equation of state $e = 3P$, where e is the internal energy density and P is the pressure of the fluid (we use units in which the velocity of light is unity). In this case, the sound speed of the gas is constant, with a value $v_s = 1/(3)^{1/2}$, and the proper sound speed is $c_s = \gamma_s v_s = 1/(2)^{1/2}$, where $\gamma_s = (1 - v_s^2)^{-1/2}$ is the Lorentz factor of the relativistic gas. In addition, the flow is assumed to be adiabatic, steady, cylindrically symmetric, and irrotational. Under these conditions, we obtain two quasilinear, partial differential equations which

[1] Also Institute of Astronomy, Cambridge, England.

describe the flow velocity as a function of position in the jet. These equations may be reduced to four first-order ordinary differential equations using the method of characteristics (see Courant and Friedrichs 1948 for an excellent summary of this technique), which may be solved numerically to obtain the velocity of the gas as a function of position in the jet. Once the velocity is known at a particular point within the jet, the pressure (and hence internal energy) may be obtained using the relativistic analog of Bernoulli's equation.

We begin with the relativistic equations of motion for a fluid (see, for example, Landau and Lifshitz 1959). The equation of energy and momentum conservation reads

$$\frac{\partial T_i^k}{\partial x^k} = u_i \frac{\partial}{\partial x^k}(wu^k) + wu^k \frac{\partial u_i}{\partial x^k} + \frac{\partial P}{\partial x^i} = 0 , \tag{1}$$

where $T_{ik} = wu_i u_k + Pg_{ik}$ is the energy-momentum tensor, u^i is the four-velocity of the fluid, $w = e + P$ is the heat function per unit volume (measured in the rest frame of the fluid), e is the internal energy density, P is the pressure of the fluid (both measured in the rest frame of the fluid), and g_{ik} is a tensor with off-diagonal components equal to zero: $g_{xx} = g_{yy} = g_{zz} = 1$ and $g_{tt} = -1$. Multiplication of equation (1) by u^i yields

$$-\frac{\partial}{\partial x^k}(wu^k) + u^k \frac{\partial P}{\partial x^k} = 0 . \tag{2}$$

The continuity equation is

$$\frac{\partial}{\partial x^i}(nu^i) = 0 , \tag{3}$$

where the number density n is measured in the rest frame of the fluid and we assume that there is no destruction or production of particle pairs. Using the relation $u_i = \Gamma(v_i, 1)$, where v_i, $i = 1, 2, 3$ are the three space components of the velocity, and $\Gamma = (1 - v^2)^{-1/2}$ is the Lorentz factor of the bulk flow velocity, the above relations reduce to

$$v_i \frac{\partial P}{\partial t} + \frac{\partial P}{\partial x_i} + w\Gamma^2\left[(\boldsymbol{v} \cdot \nabla)v_i + \frac{\partial v_i}{\partial t}\right] = 0 , \tag{1a}$$

$$w\left[(\nabla \cdot \boldsymbol{v}) + \Gamma^2 \boldsymbol{v} \cdot (\boldsymbol{v} \cdot \nabla)\boldsymbol{v} + \Gamma^2 \boldsymbol{v} \cdot \frac{\partial \boldsymbol{v}}{\partial t}\right] + (\boldsymbol{v} \cdot \nabla)e + \frac{\partial e}{\partial t} = 0 , \tag{2a}$$

and

$$\frac{\partial n}{\partial t} + (\boldsymbol{v} \cdot \nabla)n + n\left[(\nabla \cdot \boldsymbol{v}) + \Gamma^2 \boldsymbol{v} \cdot (\boldsymbol{v} \cdot \nabla)\boldsymbol{v} + \Gamma^2 \boldsymbol{v} \cdot \frac{\partial \boldsymbol{v}}{\partial t}\right] = 0 . \tag{3a}$$

Three reasonable assumptions greatly simplify these equations. The assumption that the flow is adiabatic implies that $Pn^{-\hat{\gamma}} =$ constant, where $\hat{\gamma}$ is the adiabatic index. In addition, the assumption that the gas is relativistic yields $e = 3P$ and $\hat{\gamma} = 4/3$. For a steady flow, $\partial/\partial t \to 0$ and equation (1) reduces to Bernoulli's equation:

$$(\boldsymbol{v} \cdot \nabla)\Gamma P^{1/4} = 0 . \tag{5}$$

We also find that

$$(\boldsymbol{v} \cdot \nabla)P + 2P(\nabla \cdot \boldsymbol{v}) = 0 . \tag{6}$$

Equations (5) and (6) imply that

$$\Gamma(\nabla \cdot \boldsymbol{v}) - 2(\boldsymbol{v} \cdot \nabla)\Gamma = 0 . \tag{7}$$

The three-dimensional flow is assumed to be cylindrically symmetric. In cylindrical coordinates, with the z-direction along the axis of symmetry of the jet and the r-axis perpendicular to the z-axis (see Fig. 1), equation (7) becomes

$$\frac{\partial v_r}{\partial r}(1 - M_r^2) + \frac{\partial v_z}{\partial z}(1 - M_z^2) - M_r M_z\left(\frac{\partial v_z}{\partial r} + \frac{\partial v_r}{\partial z}\right) + \frac{v_r}{r} = 0 , \tag{8}$$

where V_x is the component of the velocity parallel to the axis of symmetry of the cylinder, v_r is that perpendicular to the z-axis and, following Königl (1980), $M_\alpha = \Gamma v_\alpha / c_s$. For an irrotational flow

$$\nabla \times \boldsymbol{v} = \frac{\partial v_r}{\partial z} - \frac{\partial v_z}{\partial r} = 0 . \tag{9}$$

Equations (8) and (9) are of the form which may be solved using the method of characteristics (Courant and Friedrichs 1948; Owczarek 1964). These two equations are used to obtain four first-order ordinary differential equations, known as characteristic equations, which describe the flow velocity of the gas in the jet.

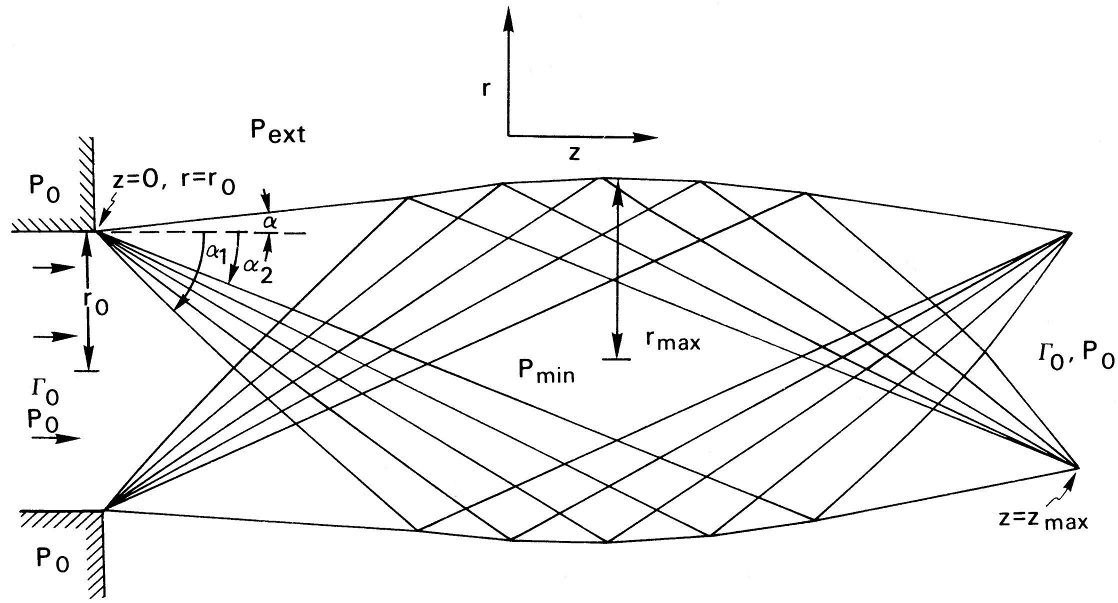

FIG. 1.—Geometry of a relativistic jet emerging from an opening into a region of lower ambient pressure. Curves fanning out from the corners are characteristics. The jet shown corresponds to the parameters $P_{\rm ext} = 0.5P_0$ and $\Gamma_0 = 1.5$. The length of the jet increases linearly with Γ_0 since the scaling law for $z_{\rm max}/r_0$ (eq. [25b]) shows that $z_{\rm max} \propto \Gamma_0/(P_{\rm ext}/P_0)$.

Following Courant and Friedrichs (1948, p. 41), we employ the method of characteristics and obtain the four characteristic equations

$$\frac{dr}{dz} = \frac{M_r M_z \pm (M^2 - 1)^{1/2}}{M_z^2 - 1}, \tag{10a}$$

and

$$\frac{dv_r}{dv_z} = \frac{-M_r M_z \mp (M^2 - 1)^{1/2}}{M_r^2 - 1} + \frac{v_r}{r(M_r^2 - 1)}\frac{dr}{dv_z}, \tag{11a}$$

where $M^2 = M_r^2 + M_z^2$ and the $+(-)$ sign corresponds to the C^+ (C^-) characteristic. These equations are the same as those of Königl (1980). The four equations contained in equations (10a) and (11a), subject to boundary conditions, may be solved numerically to determine $v_r(r, z)$ and $v_z(r, z)$. We may then determine the pressure $P(r, z)$, and hence the internal energy density $e(r, z)$, using equation (5), which indicates that the quantity $\Gamma P^{1/4}$ remains constant along a streamline, with the initial value of this quantity set by the boundary conditions. In order to solve equations (10a) and (11a) along with equation (5), we impose the following boundary conditions (see last paragraph, this section): upstream of the position $z = 0$ (at which the gas flowing along the jet boundary first encounters a drop in the external pressure), the flow has a velocity and pressure independent of r; the velocity of this initial flow is in the z-direction, and pressure equilibrium is maintained between the jet boundary and the external medium.

Equations (10a) and (11a) may be further simplified. Let θ be the angle which the flow velocity makes with the symmetry axis of the jet (the z-axis); then $v_z = v \cos\theta$ and $v_r = v \sin\theta$, where $v^2 = v_r^2 + v_z^2$. Following Königl (1980), we define the relativistic Mach angle μ such that $\sin\mu = 1/M = c_s/(\Gamma v)$, where the proper sound speed of the gas is $c_s = 1/(2)^{1/2}$. Equations (10a) and (11a) then become

$$\frac{dr}{dz} = \tan(\theta \pm \mu), \tag{10b}$$

and

$$d\theta = \pm\frac{dv}{v}\cot(\mu) \mp \frac{1}{\cot(\mu) \pm \cot(\theta)}\frac{dr}{r}. \tag{11b}$$

These are identical to the equations which describe a three-dimensional, nonrelativistic, cylindrically symmetric flow (Owcarek 1964; Königl 1980). Equation (11b) may also be written as

$$d\theta = \pm dv \mp \frac{1}{\sqrt{(M^2 - 1)} \pm \cot(\theta)}\frac{dr}{r}, \tag{11c}$$

where the $\pm$ signs correspond to the C^+ and C^- characteristics and

$$dv = \frac{\sqrt{(M^2 - 1)}}{M(1 + M^2/2)} dM . \tag{12}$$

Equation (12) may be solved analytically, yielding

$$v = \sqrt{3} \arctan \sqrt{\frac{M^2 - 1}{3}} - \arctan \sqrt{M^2 - 1} . \tag{13}$$

The equations describing a two-dimensional flow are equation (10b), along with

$$d\theta = \pm dv . \tag{11d}$$

In general, the second term on the right-hand side of equation (11c) is small relative to the first term. Hence, the three-dimensional equation (11c) describing $d\theta$ (the change in the direction of the flow velocity) is quite close to the two-dimensional equation (11d); the three-dimensional equation only differs from the two-dimensional equation by a small correction term—the second term on the right-hand side of equation (11c).

To summarize, equations (10b) and (11c) are the characteristic equations which describe the flow velocity in a three-dimensional, irrotational, cylindrically symmetric, steady jet. The internal energy of the gas in the jet is assumed to be ultrarelativistic (mean total energy per particle much greater than the rest mass energy), and the flow is assumed to be adiabatic and supersonic (and therefore relativistic) at all points in the jet. Once these equations have been solved to obtain the flow velocity of the gas as a function of position in the jet, the pressure of the gas as a function of position in the jet may be obtained from equation (5).

If the flow is two-dimensional, equation (11c) is greatly simplified and reduces to equation (11d). Both the two- and three-dimensional equations describing an axisymmetric, relativistic flow of a gas described by a relativistic equation of state (eq. [10b] along with eqs. [11c] and [11d]) are identical in form to the two- and three-dimensional equations (respectively) describing a nonrelativistic, axisymmetric flow of a gas described by a nonrelativistic equation of state (Königl 1980). It is known that, in the nonrelativistic case, the solutions to the two- and three-dimensional equations of motion are nearly identical (Courant and Friedrichs 1948). Hence, we expect the solutions to the two-dimensional relativistic equations of motion to be good first-order approximations to the solutions of the three-dimensional equations of motion. In fact, this can be seen by comparing equations (11c) and (11d). The second term on the right-hand side of equation (11c) is small relative to the first term, and may be considered to be a correction to the first-order approximation (given by the first term on the right-hand side of eq. [11c] and equal to the right-hand side of eq. [11d]).

A finite difference scheme similar to that used by Owczarek (1964) is employed to solve equations (10b) and (11d) for the two-dimensional flow. It is very straightforward to solve the two-dimensional equations numerically. This is because, in the two-dimensional case, the equations (10b) and (11c) decouple; we may solve equations (11d) for θ and then use this value of θ in equations (10b) to solve for r and z. However, in the three-dimensional case equations (10b) and (11c) do not decouple, and we must simultaneously solve these equations for θ, r, and z. The numerical solutions require several iterations for each characteristic. The iterations often become unstable, especially in the interesting case of small pressure ratios $P_{\text{ext}}/P_0 \lesssim 0.7$. For these reasons the analysis here is carried out for the two-dimensional (2D) case despite the fact that real jets are three-dimensional (3D). Since, as is noted above, 2D and 3D numerical simulations of jets are found to produce very similar results, we do not consider this to limit the application of our calculations to real jets.

The boundary conditions on the jet are as follows (see Fig. 1). A cylindrical flow with zero opening angle is in pressure equilibrium with its surroundings, at pressure P_0. The bulk flow velocity of the gas in the jet is constant across a cross-sectional area (plane of constant z) of the jet for values of $z \leq 0$, that is, there are no velocity or pressure gradients along the radial direction of the jet at positions with $z \leq 0$. The bulk flow Lorentz factor is $\Gamma_0 = (1 - v_0^2)^{-1/2}$, at positions corresponding to $z \leq 0$. At positions $z > 0$ the pressure confining the jet is $P_{\text{ext}} < P_0$, and $P_{\text{ext}} = \text{constant}$. The flow velocity vector at all points downstream from the $z = 0$ plane depends only upon the ratio P_{ext}/P_0 and Γ_0. Equation (5) indicates that $\Gamma P^{1/4}$ is constant along a streamline; hence, $\Gamma P^{1/4} = \Gamma_0 P_0^{1/4}$. Once the bulk flow velocity is known at a given point in the jet, the pressure and, through the equation of state, the density, are also known. The pressure of the fluid elements along the boundary of the jet is constant at a value equal to P_{ext}. Hence, the bulk flow Lorentz factor for fluid elements which define the boundary of the jet is constant and is given by $\Gamma_e = \Gamma_0(P_0/P_{\text{ext}})^{1/4}$. Fluid elements in the interior of the jet are accelerated and decelerated as they cross characteristics. The fluid elements are accelerated when they enter a region of lower pressure, viz., as they cross the "opening fan" of characteristics and are decelerated as they enter regions of higher pressure, viz., as they cross the "closing fan" of characteristics. The pressure is minimized, and hence the velocity is maximized, in the central region at a value P_{min} (see Fig. 1).

III. RESULTS

The shape of the boundary of the jet and the bulk flow velocity, pressure, and internal energy density of the gas in the jet depend upon only two parameters: the initial bulk Lorentz factor Γ_0 and the ratio of the external pressure to the initial pressure of the gas in the jet, P_{ext}/P_0. Once these boundary conditions (Γ_0 and P_{ext}/P_0) have been specified, the characteristic equations (10b) and (11d) may be solved numerically. The results can be scaled to a jet of arbitrary size by adopting appropriate units for the initial cross-sectional radius r_0. To illustrate the dependence of the jet characteristics on the parameters Γ_0 and P_{ext}/P_0, which we parameterize by $\xi = [(P_{\text{ext}}/P_0)]^{1/2}$, we give the scaling laws for the following jet properties as functions of ξ and Γ_0: (*a*) the opening half-angle of the jet α, and the angles α_1 and α_2 which characterize the paths of Mach waves traveling inward toward the symmetry axis of the jet from the point on the jet boundary where the pressure is discontinuous (see Fig. 1); (*b*) the pressure in the most

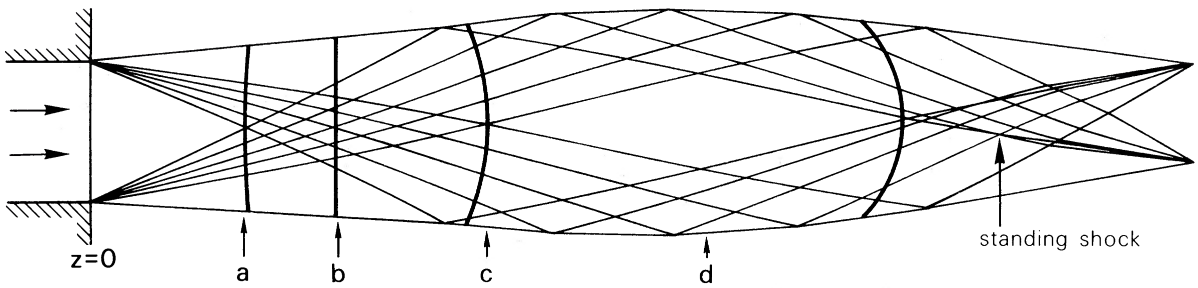

FIG. 2.—Illustration of the typical flow pattern of a relativistic jet for cases in which the external pressure is less than half the initial pressure of the jet. Formation of a standing shock is indicated by the crossing of characteristics in the downstream region. Thick curves drawn across the jet correspond to the shape of a feature initially transverse to the jet axis and moving with the background jet flow. Transverse sections across which the flow parameters are calculated in Fig. 3 are indicated by the letters and arrows. The parameters of the jet shown are $P_{ext} = 0.4P_0$ and $\Gamma_0 = 2.0$.

rarefied region of the jet P_{min} (see Fig. 1); (*c*) the maximum width of the jet r_{max} (see Fig. 1); (*d*) the length scale of the jet as measured by the distance z_{max} between the point of the pressure drop (located at $z = 0$) and the next minimum in the cross-sectional area of the jet (see Fig. 1); and (*e*) the highest value of ξ at which shocks occur in the jet (see Fig. 2).

The following relations are useful. The Mach number of the flow M is given by

$$M^2 = 2v^2\Gamma^2 = 2(\Gamma^2 - 1) . \tag{14}$$

The Mach angle of the flow μ is given by

$$\sin(\mu) = \frac{1}{M} . \tag{15}$$

Bernoulli's equation implies that, along a streamline, $\Gamma P^{1/4}$ is constant, or

$$\Gamma^2 = \Gamma_0^2\left(\frac{P_0}{P}\right)^{1/2} . \tag{16}$$

Hence, the Mach number is related to the pressure by

$$M^2 = 2\left(\Gamma_0^2\sqrt{\frac{P_0}{P}} - 1\right) . \tag{17a}$$

We note that

$$M_e^2 = 2(\Gamma_0^2\xi^{-1} - 1) = \text{constant} \tag{17b}$$

is the Mach number of the flow along the boundary of the jet at positions $z > 0$. For regions in which the pressure P is small relative to the initial pressure in the jet P_0 and/or if Γ_0 is large, the Mach number is related to the pressure by

$$M^2 \approx M_0^2\left(\frac{P_0}{P}\right)^{1/2} . \tag{17c}$$

The characteristic curves represent Mach waves which transmit pressure changes into the gas. The physical parameters ("state") of the gas remain constant up to the point where the flow is crossed by a characteristic. An abrupt change in the boundary conditions of the flow results in a "fan" of characteristics which emanate from the position of the abrupt change. In Figure 1 we represent this fan by five upper (C^-) and five lower (C^+) characteristics, the interior three of which in each case are arbitrarily selected from a continuum of characteristics. The innermost characteristic is initially inclined at an angle α_1 to the initial flow direction (normal to the $z = 0$ plane), while the outermost characteristic is initially inclined at an angle α_2 to this direction (see Fig. 1). The streamline along the boundary of the jet subtends an initial angle α to the initial direction of the flow. The angle α_1 is the initial Mach angle; the angle α_2 is the Mach angle at the boundary minus α (see § III*a* below).

The jet expands upon entering the region of lower pressure, then overexpands (because of the inertia of the inner, higher velocity regions), and finally contracts since the expansion Mach waves reflect off the boundary as compression waves. The latter is a result of the higher pressure at the boundary P_{ext} relative to the central pressure P_{min}. The jet therefore reconverges to its initial state. Beyond this point the jet reexpands in a similar fashion such that the jet has a repeating pattern of oscillating cross section.

This qualitative picture breaks down for very low values of P_{ext}/P_0 ($\lesssim 0.5$). In these low-pressure cases, the reflected compression waves converge to form standing oblique shocks and possibly Mach disks (strong, transverse, standing shocks near the axis of the jet; see Courant and Friedrichs 1948). For even lower external pressures, the expansion waves are intercepted by oblique shocks so as not to overrarefy the flow near the jet axis. This is discussed in § III*e* below.

a) *Opening Angle of the Jet*

The opening angle α of the jet boundary at the plane $z = 0$ is given by

$$\alpha = \nu_e - \nu_0 \,, \tag{18}$$

where the subscript e refers to the streamline along the boundary of the jet (at positions in the jet with $z > 0$), where the gas is in pressure equilibrium with the external medium. Equation (13) implies that

$$\nu_0 = \sqrt{3} \arctan \sqrt{\frac{M_0^2 - 1}{3}} - \arctan \sqrt{M_0^2 - 1} \,, \tag{19a}$$

and

$$\nu_e = \sqrt{3} \arctan \sqrt{\frac{M_e^2 - 1}{3}} - \arctan \sqrt{M_e^2 - 1} \,. \tag{19b}$$

Given Γ_0 and $\xi^2 = P_{ext}/P_0$, M_0 and M_e may be obtained from equations (14) and (17b); hence, α may be determined. The angle α_1 (see Fig. 1) is given by

$$\alpha_1 = \mu_0 \,, \tag{20}$$

and the angle α_2 is given by

$$\alpha_2 = \mu_e - (\nu_e - \nu_0) \,. \tag{21}$$

b) *Region of Lowest Pressure in the Jet*

The pressure P_{min} in the central, most rarefied region of the jet (see Fig. 1), may be obtained through a series of substitutions. Once the value of ν is known in this region, the Mach number M may be obtained by solving the transcendental equation (13). Once M is known, the pressure may be found from equation (17a). The value of ν is this region, $\nu(P_{min})$, is

$$\nu(P_{min}) = 2\nu_e - \nu_0 \,. \tag{22}$$

The angles ν_0 and ν_e may be obtained from equations (19a) and (19b). It is not possible to solve equation (13) analytically to obtain the pressure P_{min} in this rarefied region. However, an excellent analytic approximation to the pressure in this region may be obtained by expanding the arctangents in the expressions for, ν_e, and ν_0. We find that the pressure in the rarefied region is given by

$$\frac{P_{min}}{P_0} \approx (2\sqrt{\xi} - 1)^{1/4} \,; \tag{23}$$

this approximation is accurate to better than one part in 500. Note that the pressure in this region of the jet is independent of the initial bulk flow Lorentz factor Γ_0. As is implied by this expression, the method of characteristics breaks down for values of $P_{ext} < 0.063 P_0$ owing to the formation of shocks which "intercept" the Mach waves (see Courant and Friedrichs 1948). The formation of shocks is signaled in the numerical calculations when two C^+ or two C^- characteristics cross each other; at this point the method of characteristics breaks down.

c) *Maximum Width of the Jet*

The maximum width of the jet (r_{max} in Fig. 1) is very insensitive to the initial bulk flow Lorentz factor Γ_0. An analytic approximation can be obtained if the Mach waves are drawn as straight lines and the arctangents are again represented by a truncated series expansion:

$$\frac{r_{max}}{r_0} \sim 1 + 1.9\left[\frac{(1 - \sqrt{\xi})}{(2\sqrt{\xi} - 1)}\right] . \tag{24}$$

The second term in this expression is accurate to within $\sim 10\%$, with accuracy increasing for higher values of Γ_0 and lower values of $\xi = (P_{ext}/P_0)^{1/2}$.

d) *Characteristic Length Scale of the Jet*

We define the distance z_{max} to be the distance along the z-axis of the jet between positions on the jet where the width of the jet is a minimum (see Fig. 1). For constant external pressure, this translates into the distance from the throat of the jet (defined by the $z = 0$ plane) to the next "node" on the jet—that is, to the first constriction of the jet, or, from one constriction to the next. At this latter point the jet returns to the state which exists at the throat, i.e., $P = P_0$ and $\Gamma = \Gamma_0$ (assuming that P_{ext} is constant). Using approximations similar to those described in § III*c*, we find that, to a good approximation

$$\frac{z_{max}}{r_0} \sim \left(\frac{3.9\sqrt{2}\Gamma_0}{2\sqrt{\xi} - 1}\right) . \tag{25a}$$

This yields values for z_{max} which are accurate to within $\sim 20\%$ of those obtained numerically, again with accuracy increasing for higher values of Γ_0 and lower values of P_{ext}/P_0. In addition, we find that

$$\frac{z_{max}}{r_0} \sim 3.3\left(\frac{\Gamma_0}{\xi^2}\right) \tag{25b}$$

for $P_{ext}/P_0 \gtrsim 0.15$. (The two expressions are nearly equal for $0.15 < P_{ext}/P_0 < 0.3$; below this range expression [25a] is highly accurate, while at higher pressures both expressions are accurate to within $\sim 20\%$ and an average of the two gives the most accurate fit.)

e) Shock Formation in the Jet

Shocks form in the jet when the ratio P_{ext}/P_0 falls below a critical value. The formation of shocks within the jet is signaled when two adjacent characteristics intersect each other, as described at the end of § III*c*. As the value of ξ drops shocks begin to form in the closing fan angle of the jet at z coordinates approaching z_{max} (see Fig. 2). (In three dimensions these standing oblique shocks are connected by a Mach disk; see Courant and Friedrichs 1948.) As P_{ext}/P_0 decreases further, the z coordinate at which the shocks begin to form decreases; the shock formation occurs "earlier," at points farther upstream from z_{max}. The maximum value of P_{ext}/P_0 at which shock formation occurs is ~ 0.5; in this case the shocks form in the closing fan of the jet. Shock formation does not result for situations in which P_{ext}/P_0 is > 0.5 and always occurs for $P_{ext}/P_0 < 0.5$. The smaller the value of P_{ext}/P_0, the farther upstream from the closing fan angle the shocks form. Note that shock formation is independent of Γ_0. Figure 2 shows the paths of Mach waves in a jet with $P_{ext}/P_0 = 0.4$ and $\Gamma_0 = 2.0$. Note the crossing of the Mach lines in the downstream region of the jet. This indicates the formation of a standing oblique shock at this location in the jet.

IV. DISCUSSION

a) External Pressure Gradients

Although the results of the previous section apply to a particular idealized flow problem, we can extend the physical insight gained to the general problem of compact relativistic jets thought to exist in quasars and active galactic nuclei. For example, the pressure drop might be more gradual than the abrupt change adopted above (although the pressure drop could be rather sharp in the case of magnetically confined jets). As discussed by Begelman, Blandford, and Rees (1984), a pressure gradient steeper than $P_{ext} \propto z^{-2}$ is an abrupt drop in that the jet parameters cannot vary smoothly along the boundary. If the gas does not go into free expansion then a series of rarefactions and compressions occurs, similar to the case of a sudden pressure drop. In this case, expansion and compression waves are emitted at every point along the boundary. The resulting characteristic pattern is therefore quite complex. If the pressure gradient is not too steep, the jet still reconverges, although to a *local* minimum cross section which is greater than the cross section at the throat ($z = 0$). The jet pattern is then oscillatory with z_{max} and r_{max} increasing in successive sections. If the external pressure were to drop off more slowly than $P_{ext} \propto z^{-2}$, r_{max} would increase more slowly than z_{max}, leading to collimation of the jet (see Begelman, Blandford, and Rees 1984); the opposite would be the case if P_{ext} were to drop off more rapidly than this. In the limit in which the characteristic length scale of the pressure gradient greatly exceeds z_{max}, however, P_{ext} is nearly constant across each section of the jet, and the jet pattern is nearly identical to that described in §§ II and III above. The values of z_{max} and r_{max} slowly increase outward in this case.

In the event that VLBI observations become capable of determining jet characteristics such as the opening half-angle of the jet, the width of the jet, or the scale length of the jet, the boundary conditions of the jet (Γ_0 and P_{ext}/P_0) could be estimated. In this way, oscillating compact jets would serve as probes of the media surrounding them, as described in detail in §§ IV*c*(i) and IV*c*(iv).

b) Velocity Gradients: Evolution of a Feature in the Jet

Most of the results of the previous section are quite similar to those obtained for nonrelativistic jets. As pointed out by Königl (1980) and Wilson (1987), the nonrelativistic and relativistic equations governing the pattern of characteristics are identical when cast in the form presented in § II. One important practical difference is that, by definition, the velocities are close to the speed of light in a supersonic, relativistic jet. This leads to beaming of the emission and effects due to light travel time delays. Velocity gradients across the jet therefore affect the geometry of emission features observed in the jet.

Since the Lorentz factor (and hence velocity) depends on the local pressure in the jet (see eq. [16]), the existence of pressure gradients causes velocity gradients to occur as well. In Figure 3 we illustrate the pressure and Lorentz factor variations across the jet for several values of z, for the jet shown in Figure 2 (as described in the next paragraph). Since the interior of the jet is unaffected by the drop in external pressure up to a point downstream of the drop, the boundary of the jet is accelerated first. Once the rarefaction reaches the interior region, however, the flow along the axis becomes more rarefied, and hence attains a higher velocity than the outer region. At the central, most rarefied region, the velocity along the axis is substantially higher than that along the boundary.

A simple example illustrates this effect nicely. Consider the jet shown in Figure 2, which has $\Gamma_0 = 2.0$ and $P_{ext}/P_0 = 0.4$. We follow the geometrical evolution of an infinitesimally thin feature which is, at the plane $z = 0$, transverse to the direction of flow. This feature is then imagined to move at the same velocity as the background jet flow (which allows one to see the effects of velocity gradients within the jet). For low values of z, the center of the feature lags somewhat behind the outer edge. By the time the feature reaches the central, most rarefied region, however, the center is ahead of the outer edges. This becomes more pronounced until the compression waves are reached, beyond which point the center decelerates to the initial velocity. Nevertheless, because of its higher speed over most of the jet, the center reaches the plane $z = z_{max}$ well ahead of the outer regions. (This cannot be illustrated in Fig. 2 owing to the onset of shocks at $z \lesssim z_{max}$.) An initially transverse feature is therefore distorted by the velocity gradients across the jet.

The above discussion ignores the effects of light-travel time delays in the observer's frame; these are important because of the relativistic speed of the jet flow. The magnitude of these effects depends on the velocity gradients as well as on the viewing angle of

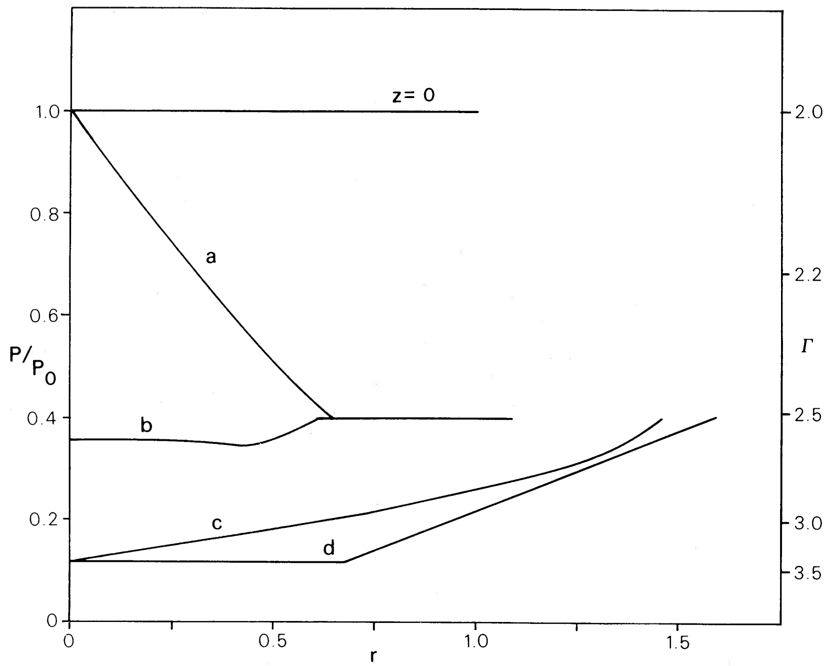

FIG. 3.—Pressure and Lorentz factor gradients in the direction transverse to the jet axis for the jet of Fig. 2. Letters correspond to sections of the jet marked in Fig. 2. The value of r_0 has been set equal to unity (i.e. $r/r_0 \rightarrow r$) in this figure.

the observer. If the jet is viewed at an angle less than $\sim 20°$ from the axis, as required in relativistic jet models for superluminal motion, a simple calculation shows that the outer edge of the feature over the entire circumference lines up (i.e., appears edge-on) while the central region lags behind or moves ahead of the outer edge, as described above.

c) Comparison with Real Jets: Superluminal Radio Sources

i) *Application of Our Calculations to Observed Jets*

Past interpretations of the compact jets observed in extragalactic radio sources have been based primarily on simplified geometries which ignore the complications introduced by various possible flow patterns. The most common assumption, chosen because it greatly reduces the number of free parameters, is that the jet is conical, with gradients in the physical parameters allowed only in the z-direction. While it is possible for such a geometry to exist (see § IV*d* below and Fig. 5, part I), the flow pattern is more complicated if the gas in the jet has a relativistic internal energy in the region of interest.

To calculate the observed emission pattern of a relativistic compact jet would require inclusion of beaming effects and particle acceleration as well as the gas dynamics discussed here. This should be done once our calculations are extended using a complete numerical fluid dynamics code, but is beyond the scope of the present paper. Nevertheless, we can discuss qualitatively how the gasdynamical results might apply to real jets.

It is straightforward to use the scaling laws of § III to obtain the opening half-angle of a relativistic jet which encounters a region of lower external pressure (see eq. [18]). Furthermore, it is a simple matter to use Figures 1, 2, and 3 to interpret jet flows with higher or lower upstream Lorentz factors Γ_0: the dominant effect of higher values of Γ_0 is to "stretch out" the jet (see expressions [25a] and [25b]). This is caused by relativistic aberration. The effects of varying external pressure are also given in § III.

There are two limitations to the application of our results to observed jets. The first is the unknown orientation of an observed jet to the observer. A jet of opening half-angle α and inclination of axis to the line of sight ϕ has an apparent opening half-angle equal to arctan (tan α cot ϕ). Hence, unless ϕ is known, the opening half-angle α cannot be determined. The apparent speed (relative to the speed of light, c) of an observed feature in the jet moving at the jet flow Lorentz factor Γ is given by $v_{\rm app} \approx v \sin \phi/(1 - v \cos \phi)$ (we use units in which $c = 1$). Hence, there are three parameters to be determined, Γ_0, ξ, and ϕ, and two observable quantities, α and $v_{\rm app}$; more observables may become available, as described below. In addition, one must assume that the speed of a feature is equal to the flow speed of the jet and that the features used to obtain α extend across the entire width of the jet. Nevertheless, if one is willing to work under these assumptions and limit the range of ϕ to that value which minimizes Γ, the values of Γ_0, ξ, and ϕ can, in principle, be estimated. If the value of $(z_{\rm max} \sin \phi)/(r_0 \cos \phi)$ can be obtained from VLBI observations, then expressions (25a) and (25b) can be used to provide an additional constraint, thereby allowing one to avoid the need to assume an optimum value of ϕ. Since the compact "cores" are typically unresolved by Earth-based VLBI, the value of r_0 cannot be determined in most sources at present. Space-based VLBI antennas should overcome this problem in the future. An example of how the scaling laws may be used to determine the characteristics of the surrounding medium is given in § IV*c*(iv).

The other limitation is that the method of characteristics breaks down at the point where shocks form. Hence, application of our numerical results is limited to modest pressure ratios $P_{\rm ext}/P_0$. Rather than allow this difficulty to restrict our discussion severely, in what follows we combine our calculations with a more speculative description of how we expect the flow to develop in a relativistic

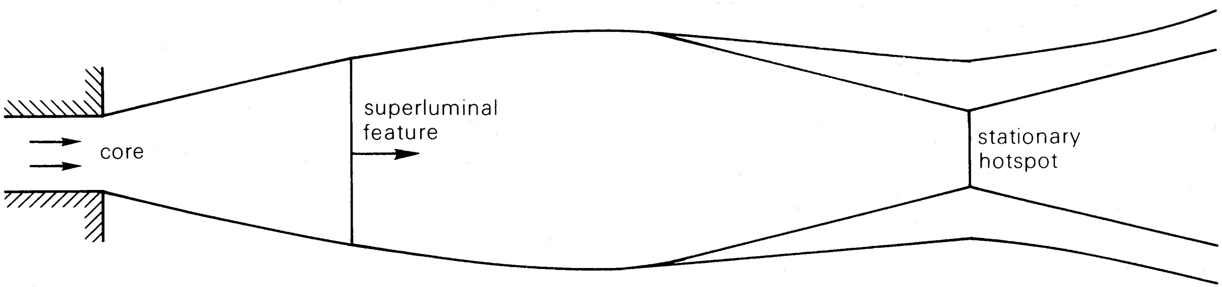

FIG. 4*a*

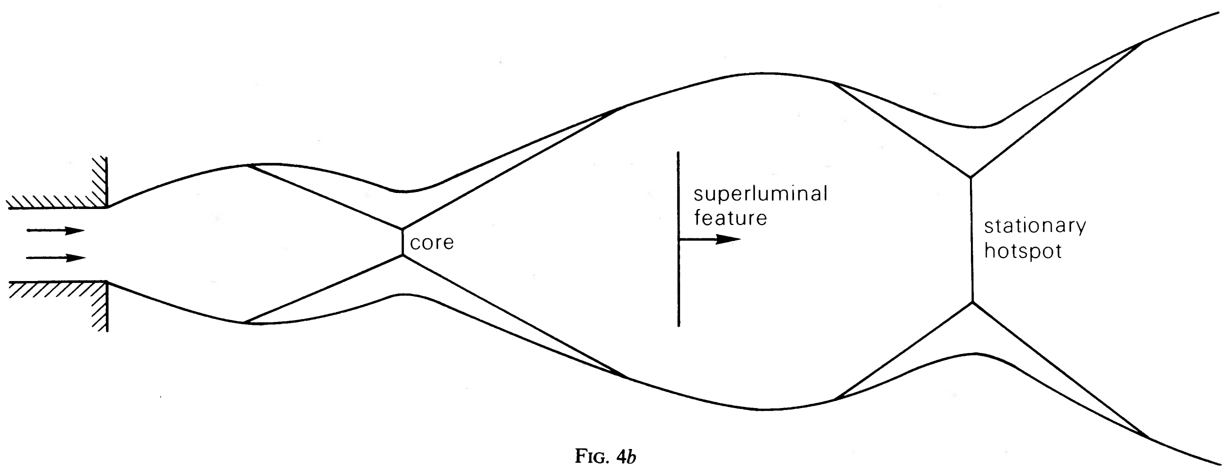

FIG. 4*b*

FIG. 4.—Two possible geometries of a compact three-dimensional core-jet radio source in which the external pressure falls off gradually beyond the opening. (*a*) The core is located at the throat of the jet where the density and magnetic field strength are relatively high. A stationary hotspot can appear at the constriction. If the external pressure gradient is not strong, the shock/Mach disk shown in the figure might be absent. (*b*) The external pressure gradient is steeper. The core is identified with the first standing shock/Mach disk system, while the stationary hotspot occurs at the second such system.

jet. These speculations are based on experience with nonrelativistic flows, as discussed by Courant and Friedrichs (1948), and the known properties of relativistic gases.

ii) *Identification of the Compact Radio Core*

One particular problem in the interpretation of observed compact jets lies in the identification of the jet feature which corresponds to the VLBI radio core. The core is the most compact feature in VLBI maps, is stationary (Bartel *et al.* 1986) and is situated at one end of the jet. In the standard jet model of Blandford and Königl (1979), the core is identified with the throat of a diverging, conical jet, where the density and magnetic field are the highest. The geometry would be similar to Figure 4*a*, except that the stationary hotspot caused by recollimation shocks would be absent. This would arise if the mean energy per gas particle were to drop below the rest mass energy, which would cause the flow to become approximately ballistic beyond a short distance from the throat (see § IV*d* below). The jet would then be approximately described as a cone with constant opening angle (but see § IV*d* below).

An attractive alternative to this picture is to identify the core with the first recollimation Mach disk shock system. The Mach disk and reflected shock, and perhaps the incident (or "intercepting") shock, would be relativistically strong shocks and therefore likely sites of efficient particle acceleration and magnetic field amplification. The result would be a compact, stationary, relativistically beamed, and therefore very bright, emission feature. The jet upstream of this feature might then be unobservable owing to the absence of shocks. This would explain why the source spectrum typically peaks at the frequency where the core becomes transparent: the core is the most compact observable feature in the jet.

iii) *Superluminal Knots*

The superluminal knots of observed sources move at roughly constant speed once they become well separated from the core. In general, the flow of a relativistic jet proceeds at constant speed only over regions of constant pressure. The region near the outer edge (where the density is high and the volume large, and hence where most of emission will be located) of a jet expelled into an ambient medium of constant pressure therefore moves at constant speed, with Lorentz factor Γ_e which may be obtained from equation (16). The central region lags or leads the outer edge; hence, the brightness centroid has a slightly variable velocity. Even in the presence of external pressure gradients, the Lorentz factor varies slowly: $\Gamma \propto P^{-1/4}$; for example, a pressure drop of a factor of 2 corresponds to a velocity increase of only 20%. In fact, Biretta, Moore, and Cohen (1986) have observed acceleration of a superluminal component in 3C 345 when it was close to the core. The speed of the jet fluid is also roughly constant beyond the point where it becomes ballistic (see §§ IV*b*, *d*).

Superluminal knots have been identified as clouds caught up in the jet flow (Blandford and Königl 1979), instabilities in the flow (Marscher 1980*b*), and shock waves propagating down the jet (Blandford and Königl 1979; Marscher and Gear 1985; Hughes, Aller, and Aller 1985). In the first two cases, the velocity of the knot is roughly that of the local jet flow. Forward shocks, on the other hand, usually decelerate slowly relative to the background flow. Since the background flow is relativistic and is expected to accelerate, a nearly constant velocity can occur in the observer's frame if the two effects are roughly equal. Otherwise, the superluminal features would be observed to have constant velocity only in the ballistic portion of the jet or along the boundary in a region of constant external pressure.

A major disturbance in the flow causes a strong, forward propagating shock to form. Our steady state calculations are not designed to handle such features. Nevertheless, the velocity of the shock front in the observer's frame is a superposition of the velocity of the shock front in the frame of the moving background flow and the velocity of the background flow itself. Since the undisturbed background flow was in a steady state prior to the passage of the shock, its contribution to the velocity of the shock in the observer's frame is given by the calculations described in §§ II and III.

An increase in the initial flow velocity v_0 and/or pressure P_0 over an extended time may cause not only shock formation, but also a transition to a new steady state. An increase in v_0 causes each section of the new jet to become longer, while an increase in P_0 leads to a greater opening angle and a longer, wider section. While the change in v_0 causes a new steady state to be set up almost immediately, an increase in P_0 in general takes longer to establish equilibrium. This is a result of the inertia of the external medium, which is colder and denser than the jet plasma. As the jet attempts to widen in response to the increase in P_0, the ram pressure of the external gas resists the expansion. A quasi–steady state is therefore set up in which the jet only slowly changes its initial geometry, with the external medium acting as a slowly expanding pipe which channels the jet flow. Rayleigh-Taylor instabilities at the jet boundary should then cause clouds to form in the external medium. The resulting jet flow cannot be described in the same manner as that of §§ II and III, although the method of characteristics can still be employed up to the point at which standing shocks are formed. Qualitatively, rarefaction fans would still emanate from the boundary at the pressure drop, but these would be intercepted by Mach waves or shocks (depending on the new value of P_e/P_0) which recollimate the flow to follow the boundaries.

iv) *The Quasar 4C 39.25*

Shaffer *et al.* (1987) and Marscher *et al.* (1987) have reported that the quasar 4C 39.25 contains a pair of brightness peaks of constant separation, with a superluminal knot in between. Furthermore, the component from which the superluminal knot is moving is not as compact as cores in other superluminal sources, and its spectrum peaks at a frequency more than 10 times lower than the typical turnover frequency of other VLBI cores. A ready explanation for this behavior is possible within the context of a relativistic jet emerging into a region of lower pressure.

The simplest scenario adopts the relativistic jet model depicted in Figure 4*a*. If the jet in 4C 39.25 were to encounter the pressure drop at a greater distance from the "central engine" than is typical, the jet would be wider and less dense at the throat. This would cause the core to be less compact than in other sources. The stationary hotspot, well separated from the core, would be caused by standing shocks where the flow recollimates (or, without shocks, simply a return to higher density and pressure at the first constriction). The absence of the feature in most other superluminal sources (3C 395 also has a stationary hotspot; see Waak *et al.* 1985) indicates that most jets may become ballistic within the rarefaction region beyond the core or are not dense enough at the first constriction for strong emission to appear there.

This model for 4C 39.25 provides a nice illustration of how to apply the results of § III to VLBI observations. Analysis of the data of Marscher *et al.* (1987) gives a value of 0.25 nas as the width of the jet, which corresponds to $r_0 \cos \phi$ in this model, at the western end, which we identify with the "core" in Figure 4*a*. The distance from the "core" to the eastern stationary component, which corresponds to $z_{\max} \sin \phi$ in this model, is 2.0 mas. The observations are, unfortunately, not detailed enough to allow us to determine the opening angle α. If we instead adopt an angle of inclination to the line-of-sight ϕ which maximizes the superluminal motion ($\sin \phi \approx \Gamma_0^{-1}$), expression (25b) yields $P_{\rm ext}/P_0 = \xi^2 \sim 0.4$. More refined VLBI observations made possible by the upcoming Very Long Baseline Array (VLBA) should allow a more precise calculation of the pressure drop for compact jets described by this model.

A similar model can be generated using the description of a jet adopted in Figure 4*b*. In this case, the core corresponds to the first recollimation shock system. The stationary feature would then be located at the second such system. For this to happen, the jet in most sources would then have to either become ballistic at a short distance beyond the first recollimation or expand owing to a gradient in external pressure, to prevent the appearance of a compact stationary hotspot which is not observed.

This schematic model for 4C 39.25 predicts that the superluminal feature, if a moving shock or cloud, should become more compact (unfortunately, it is currently unresolved on all VLBI maps) and brighten as it approaches the stationary hotspot. It should then pass through and emerge on the other side of the stationary hotspot, thereafter expanding and fading. If the shock is caused by a permanent change in the initial flow parameters, the position of the stationary hotspot could change somewhat after passage of the shock.

d) Broad Ballistic Jets

An intriguing possibility occurs if the external pressure drop is very large and abrupt. This could occur if the jet is confined by a circumferential magnetic field which, once it becomes too weak to confine the jet, only becomes weaker as the jet expands. It could

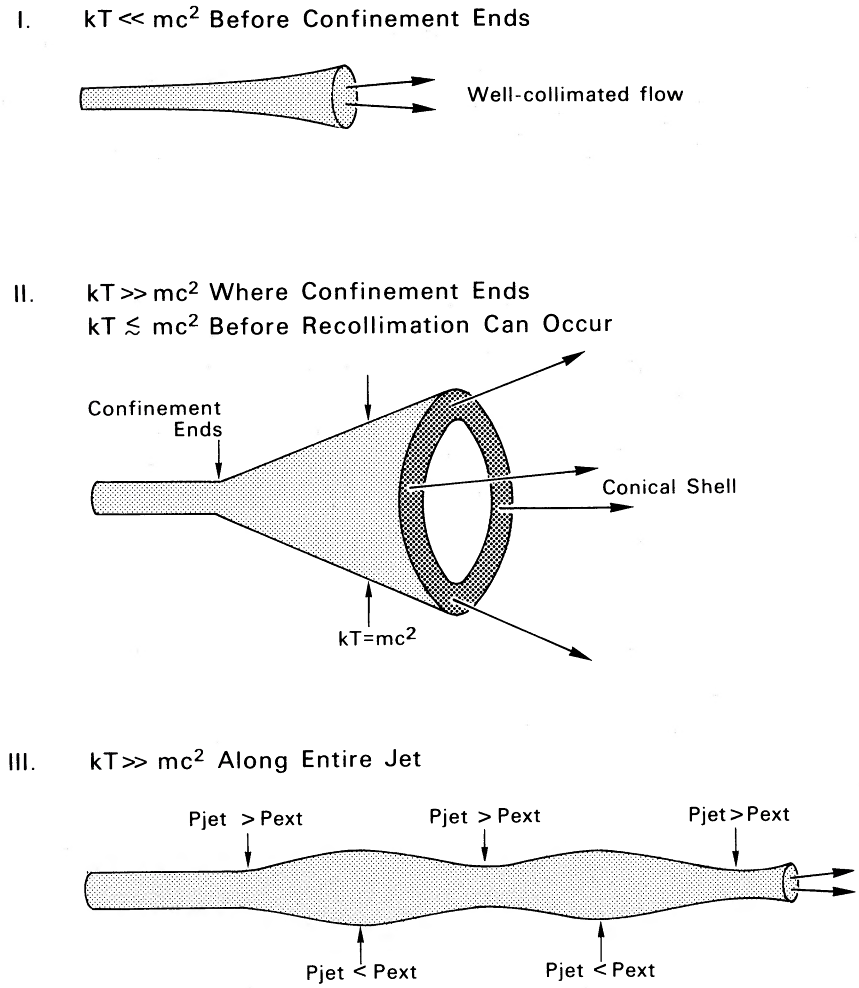

FIG. 5.—Three further possible geometries of a relativistic jet. In part I the internal energy becomes nonrelativistic before the jet can expand considerably in the lateral direction. In part II the internal energy remains relativistic when confinement ceases; this results in a broad, nearly hollow beam. In part III the external pressure is constant beyond the point where it abruptly takes on a lower value; this results in a periodic, oscillating jet. Here $P_{\rm jet}$ refers to the pressures at the axis of the jet ($r = 0$).

also occur if the external pressure gradient were to become extremely steep (as in an exponential "atmosphere" surrounding the nucleus of the host galaxy; see Sanders 1983). In this case, the opening half-angle α of the boundary (eq.[18]) can be approximated as

$$\alpha \approx \frac{\sqrt{2}}{\Gamma_0}(1 - \sqrt{\xi})\ \text{rad} \qquad (\xi \ll 1)\,, \tag{26}$$

which is accurate to within 9% for $\Gamma_0 > 1.4$, with accuracy improving at higher values of Γ_0.

The value of α can be as high as 66° for low Γ_0 and very low ξ. The extreme case of low values of Γ_0 and very steep pressure drops therefore leads to a very broad jet. Furthermore, in the rarefaction fan the flow accelerates rapidly until it becomes ballistic at a value of Γ equal to the initial mean internal Lorentz factor of the gas particles. (This occurs because the acceleration of the flow is at the expense of the internal energy of the gas.) The result is a very broad jet which is nearly hollow owing to the rarefaction of the jet interior as the flow accelerates (see Fig. 5, part II).

The concept of broad beams has been discussed previously by Rees (1981) as a possible scenario by which superluminal sources could be viewed at large angles to the jet axis. Scheuer (1984) has criticized this on the grounds that broad beams would appear as fat jets to the observer. While this would indeed be true if the jet were circularly symmetric about its axis, it need not be the case if the external pressure were to be inhomogeneous. If the point of the pressure drop were to vary with azimuthal angle, the beam would break up into a number of disconnected narrow jets whose axes subtend large angles to each other. The observer would detect the jet which beams its emission most closely toward the line of sight, with the other jets beaming in other directions. The observer might in some cases see more than one jet, which would result in a complex emission pattern (see the complex VLBI maps of some sources, e.g., 3C 147; Simon, Readhead, and Wilkinson 1984; Preuss *et al.* 1984).

The chances of detecting superluminal motion in a broad, hollow jet of opening half-angle α is enhanced by a factor $\sim\Gamma\alpha$ over that for a narrow jet. If radio source statistics prove to eliminate narrow beaming, such a model could be an attractive alternative to the standard picture. If the initial ($z < 0$) internal energy of the jet were to vary with time, the opening angle would also change, becoming smaller as the internal energy decreased. Periods of nonrelativistic initial internal energy (and higher density such that P_0 remains roughly constant) would yield a single, narrow, ballistic, nonrelativistic jet (see Fig. 5, part I). This narrow jet would be capable of feeding the extended radio lobes often seen in such sources. Since the piece of the broad relativistic jet detected by the observer can be misaligned with the true jet axis (a small misalignment amplified by projection effects as viewed by the observer), the compact jet would appear to bend toward the narrow, nonrelativistic jet and outer lobes if a long period of nonrelativistic ejection were followed by an interval of relativistic flow.

Since the opening angle of the jet is decreased as Γ_0 increases, it is also possible for the extended lobes to be fed instead during periods of *high* initial velocity, such that $\Gamma_0 \gg 1$. Such a beam could be nearly invisible if a wider channel were carved earlier by a broader jet.

V. CONCLUSIONS

The main results of our study are the scaling laws obtained for jets encountering mild drops in external pressure, and the wide variety of geometries and flow patterns possible for jets containing relativistic gas. We can divide these theoretical jets into four classes separated by the nature of the external pressure drop.

1. $0.5 \lesssim P_{ext}/P_0 \lesssim 1$, P_{ext} constant. In this case the jet encounters a mild pressure drop. The resulting pattern is a jet of oscillating cross section with no shocks. The length of each section is directly proportional to the initial Lorentz factor Γ_0, and the opening angle and length of each section depend inversely on the pressure ratio P_{ext}/P_0. Other scaling laws are detailed in § III above. A sketch of the basic geometry of the jet is given in Figure 5, part III.
2. $\langle kT/mc^2 \rangle^{-4} \lesssim P_{ext}/P_0 \lesssim 0.5$. Here $\langle kT/mc^2 \rangle$ is the initial internal energy per gas particle in units of the rest-mass energy. Jets of this type experience a severe pressure drop which results in expansion and recollimation with standing oblique shocks and Mach disks. See Figure 2 and Wilson (1987) for illustrations of this flow pattern.
3. $P_{ext}/P_0 \lesssim \langle kT/mc^2 \rangle^{-4} \ll 1$. These jets experience a severe rarefaction which causes the jet to become ballistic once the internal energy per particle drops below the rest-mass energy at the boundary. A hollow, broad beam results, as in Figure 5, Part II.
4. Gradients in P_{ext}. If P_{ext} falls off gradually with distance along the jet (as opposed to a sudden drop), the basic jet structure remains approximately the same, except that each successive section becomes wider and longer. Standing shocks occur unless the pressure gradient is very shallow. Figure 4 illustrates the basic geometry and shock pattern expected.

We call attention to the importance of the analytic expressions or scaling laws presented in § III. These were obtained by numerically solving the characteristic equations for a full range of choices for the boundary condition parameters, Γ_0 and P_{ext}/P_0. We chose aspects of the numerical solutions which best characterize the physical state of the jet (e.g. the opening half-angle, maximum width, length scale of the jet, etc.). And, we obtain the dependence of these parameters describing the physical state of the jet on the boundary conditions. This means that, given the boundary conditions (Γ_0 and P_{ext}/P_0), the gross aspects of any arbitrary jet may be determined, allowing for the assumptions introduced in deriving the characteristic equations (see § II). Conversely, if one or more gross aspect(s) of a jet may be determined observationally, the scaling laws given in § III may be used to determine or constrain the boundary conditions on the jet (see discussion in §§ IV*c*[i] and IV*c*(iv]). For example, if the pressure P_{min} in the most rarefied region of the jet, or if the maximum width of the jet is observed, the pressure ratio P_{ext}/P_0 may be obtained; if the scale length of the jet can be inferred from observations (as might be possible in the case of 4C 39.25), the initial Lorentz factor may be deduced. Similarly, observations of other aspects of a jet, such as its opening half-angle, will place constraints on the boundary conditions through the relations presented in § III.

We have used the insight obtained from our numerical results as well as known patterns of nonrelativistic jets to describe the wide range of phenomena which might be displayed by relativistic jets. Because we have often extrapolated from known solutions, the jet patterns discussed above need to be verified by 2D or 3D numerical gasdynamics codes capable of treating shocks in a proper fashion. Such calculations should allow for external pressure gradients, changes in internal energy of the gas from relativistic to nonrelativistic, and time variable flow parameters if they are to explore the full range of relativistic jet patterns which might exist in nature.

This work was supported in part by the National Science Foundation through grant AST85-16548, by NASA's Graduate Student Researchers Program, and by a NATO-NSF Postdoctoral Fellowship, Award Number RCD-8751127.

REFERENCES

Bartel, N., Herring, T. A., Ratner, M. I., Shapiro, I. I., and Corey, B. E. 1986, *Nature*, **319**, 733.
Begelman, M. C., Blandford, R. D., and Rees, M. J. 1984, *Rev. Mod. Phys.*, **56**, 255.
Biretta, J. A., Moore, R. L., and Cohen, M. H. 1986, *Ap. J.*, **308**, 93.
Blandford, R. D., and Königl, A. 1979, *Ap. J.*, **232**, 34.
Blandford, R. D., and Rees, M. J. 1978, in *Pittsburgh Conference on BL Lacertae Objects*, ed. A. M. Wolfe (Pittsburgh: University of Pittsburgh Press), p. 328.
Courant, R., and Friedrichs, K. O. 1948, *Supersonic Flow and Shock Waves* (New York: Wiley Interscience).
Hughes, P. A., Aller, H. D., and Aller, M. F. 1985, *Ap. J.*, **298**, 301.
Königl, A. 1980, *Phys. Fluids*, **23**, 1083.
———. 1981, *Ap. J.*, **243**, 700.
Landau, L. D., and Lifshitz, E. M. 1959, *Fluid Mechanics* (Oxford: Pergammon).
Marscher, A. P. 1980*a*, *Ap. J.*, **235**, 386.
———. 1980*b*, *Ap. J.*, **239**, 296.
Marscher, A. P., and Gear, W. K. 1985, *Ap. J.*, **298**, 114.
Marscher, A. P., Shaffer, D. B., Booth, R. S., and Geldzahler, B. J. 1987, *Ap. J.* (*Letters*), **319**, L69.
Norman, M. L., Winkler, K.-H. A., and Smarr, L. L. 1983, in *Astrophysical Jets*, ed. A. Ferrari and A. G. Pacholczyk (Dordrecht: Reidel), p. 227.
Owczarek, J. A. 1964, *Fundamentals of Gas Dynamics* (Scranton: International Textbook Co.).
Preuss, E., Alef, W., Whyborn, N., Wilkinson, P. N., and Kellermann, K. I. 1984, in *IAU Symposium 110, VLBI and Compact Radio Sources*, ed. R. Fanti, K. Kellermann, and G. Setti (Dordrecht: Reidel), p. 29.
Rees, M. J. 1981, in *IAU Symposium 94, Origin of Cosmic Rays*, ed. G. Setti, G. Spada, and A. W. Wolfendale (Dordrecht: Reidel), p. 139.
Reynolds, S. P., and McKee, C. F. 1980, *Ap. J.*, **239**, 893.
Sanders, R. H. 1983, *Ap. J.*, **266**, 73.

Scheuer, P. A. G. 1984, in *IAU Symposium 110, VLBI and Compact Radio Sources*, ed. R. Fanti, K. Kellermann, and G. Setti (Dordrecht: Reidel), p. 197.

Shaffer, D. B., Marscher, A. P., Marcaide, J., and Romney, J. D. 1987, *Ap. J. (Letters)*, **314**, L1.

Simon, R. S., Readhead, A. C. S., and Wilkinson, P. N. 1984, in *IAU Symposium 110, VLBI and Compact Radio Sources*, ed. R. Fanti, K. Kellermann, and G. Setti (Dordrecht: Reidel), p. 111.

Waak, J. A., Spencer, J. H., Johnston, K. J., and Simon, R. S. 1985, *A.J.*, **90**, 1989.

Wilson, M. J. 1987, *M.N.R.A.S.*, **226**, 447.

RUTH A. DALY: Department of Physics-Joseph Henry Laboratories, Jadwin Hall, Princeton University, Princeton, NJ 08544

ALAN P. MARSCHER: Department of Astronomy, Boston University, 725 Commonwealth Ave., Boston, MA 02215